Improving the Sensitivity of Unobtrusive Inactivity Detection in Sensor-Enabled Homes for the Elderly

Alvin C. Valera   Hwee-Pink Tan   Liming Bai

SMU-TCS iCity Lab, Singapore Management University, Singapore 178902

E-mail: {alvinvalera,hptan,lmbai}@smu.edu.sg

Abstract—Unobtrusive in-home monitoring systems are gaining acceptability and are being deployed to enable relatives and caregivers to remotely monitor and provide timely care to their elderly loved ones or senior clients, respectively, who are living independently. Such systems can provide information about non-movement or inactivity of the elderly resident. As prolonged inactivity could mean potential danger, several algorithms have been proposed to automatically detect unusually long durations of inactivity. Such schemes, however, suffer from low sensitivity due to their high detection latency. In this paper, we propose Dwell Time-enhanced Dynamic Threshold (DTDT), a scheme for computing adaptive alert thresholds that exploit region-specific dwell time to reduce the detection latency. Using extreme value theory, we obtain a closed form expression for the per-region alert thresholds. We perform simulations using real data to evaluate the performance of DTDT and compare it with state-of-the art schemes AID and the algorithm by Moshtaghi *et al*. Results show that DTDT shows significantly lower detection latency, 1.5–3 hours shorter, in regions with short dwell times (bathroom and kitchen) while maintaining the same false alarm rate.

I. Introduction

In Singapore and nearly all countries of the world, the population is ageing due to decreasing mortality and declining fertility [2]. Coupled with the preference of most seniors to *age-in-place*, *i.e.*, live independently, safely and comfortably in their own homes and communities [1], [3], [8], numerous *in-home monitoring systems* have been developed and deployed [4], [10], [12], [13]. These systems enable relatives and care providers to remotely monitor and provide timely care to their elderly loved ones or senior clients, respectively.

Among the multitude of in-home monitoring systems, solutions that employ non-vision-based sensors are becoming more acceptable to seniors because of their unobtrusiveness, thereby offering a sense of privacy to the residents [7], [12]. One of the most widely deployed non-intrusive sensors is the passive infra-red (PIR) sensor which can detect motion. Several studies [6], [8], [11] have focused on the use of PIR sensors to detect prolonged inactivity which could indicate that the resident encountered a potentially serious situation that rendered her immobile. In [6], [8], the authors proposed algorithms to compute dynamic alert thresholds for every individual senior using her historical inactivity data. An alert is then automatically triggered whenever the inactivity duration exceeds the alert threshold that is in effect.

The downside of relying solely on inactivity data is that the *detection latency* – the time from the occurrence of emergency event until its detection, can be considerably long. This is especially the case in situations where the elderly resident has been historically inactive for long durations, *e.g.*, at night when she is asleep. In this paper, we therefore seek to reduce the detection latency by leveraging on the *dwell times* at different parts or regions of the house. This approach hinges on the notion that there are certain regions of the house where the resident does not stay for long durations. For instance, most individuals dot not dwell for long periods in the bathroom and kitchen. We can use dwell time to shorten the alert threshold as follows: If the last known region of movement was the bathroom, then the alert threshold could be set based on the historical bathroom dwell time of the resident.

The rest of the paper is organized as follows. Section II presents a brief survey of related work. Section III provides a detailed account of the smart home environment setup that is needed to collect inactivity and dwell times. Section IV introduces the proposed scheme of enhancing the alert line using per-room dwell times. Section V presents the results of the evaluation and performance comparison. Section VI concludes the paper and highlights some important future research work.

II. Related Work

The use of sensors to monitor the condition and assess the well-being of senior citizens has been widely studied in the literature [4], [10], [12], [13]. Several authors have studied extended inactivity detection in the context of in-home monitoring systems. In [6], the authors employed statistical non-parametric approach using a specific percentile of historical inactivity (added with uniform and variable buffer time) to determine the alert threshold.

Moshtaghi *et al*. [8] extended the above work to consider the inactivity at different regions of the house. To set the threshold, they used a parametric approach whereby the inactivity data distribution is modeled as a mixture of exponential distributions. A divide-and-conquer expectation maximization was proposed to find the exponential tail and using its parameters, the alert threshold can then computed. Planinc and Kampel [10] introduced the use of activity histogram comparisons to detect unusual inactivity. A key difference is that their study made use of vision-based sensors, whereas [6] and [8] primarily used motion sensors.
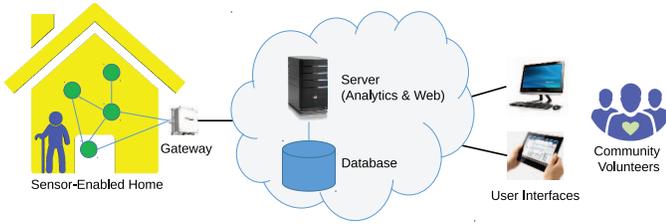
Fig. 1. Simplified view of the SHINESeniors system infrastructure.

III. Sensor-Enabled Home for Unobtrusive Monitoring

Sensor-enabled homes for a liveable community to support active ageing-in-place for senior Singaporeans is one of the major deliverables of the *SHINESeniors Project*[a]. Its ultimate aim is to develop a care model that includes a personalized care plan and an escalation protocol for each elderly resident based on their daily living patterns. To date, we have completed the installation of 50 sensor-enabled homes out of the target 100 homes.

Fig. 1 shows a simplified view of the end-to-end system infrastructure of the SHINESeniors Project, including the two key stakeholders of the system which are the elderly residents and care providers. The main technology components of the system are: (*i*) sensor-enabled home of the elderly resident; (*ii*) gateway to transmit the sensor readings from home to back-end; (*iii*) back-end servers for storage, analytics, and dissemination; and (*iv*) user interfaces in the form of web and mobile apps. The sensor-enabled home monitors the resident and in cases of abnormal behavior, the back-end sends alerts to the assigned caregivers.

A. Sensor-Enabled Home Setup

Larizza *et al.* [7] found out that seniors are generally amenable to in-home monitoring systems that are *unobtrusive* (*i.e.*, do not employ vision-based or audio-based technologies) and *require minimal action from participants*, among others. Based on this, and from the result of our own survey, we have chosen two types of non-intrusive sensors, namely, (*i*) passive infra-red (PIR) sensor and (*ii*) reed switch. The PIR sensor is used to detect motion within a region of coverage while the reed switch is used to detect main door opening and closing. In addition to being non-intrusive, these sensors do not require any action from the elderly and they do not need to change their daily activities to accommodate them.

A typical home installation is shown in Fig. 2. Note that the target participants of the SHINESeniors Project are senior citizens living alone in Housing Development Board (HDB) rental flats. A typical rental flat consists of one bedroom, one kitchen, one bathroom, and one living room. Every region/location in the home is covered by one PIR sensor, while the reed switch is attached to the main door of the unit.
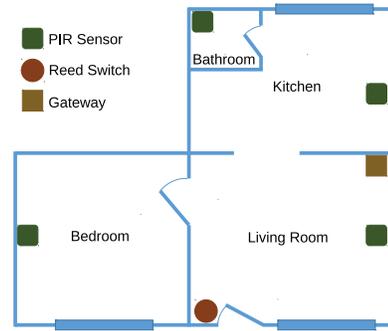
Fig. 2. Typical sensor deployment in a single bedroom rental flat.

Thus, an installation requires only 5 sensors (4 PIR sensors and 1 reed switch.) In addition to the sensors, every home is also equipped with a gateway which is responsible for relaying all sensor data to the back-end for storage and processing[b].

B. Sensor Data

The sensors are configured to sense and log their respective states once every ten seconds. Both PIR sensor and reed switch are binary sensors, which means that their state can be represented by two values:

- 0: to indicate no motion is detected for PIR, and door did not change state for reed switch; and
- 1: to indicate motion is detected for PIR and door changed state for reed switch.

The gateway aggregates the sensor logs and transmits them to the back-end once every two minutes. From these raw sensor logs, we can then derive three types of information:

1) Flat Status: Using the transitions of the reed switch state, we can reliably determine whether a flat is *empty*, *i.e.*, the resident has left the premises, or *occupied*, *i.e.*, the resident is in the premises.

2) Inactivity Time: At any time t, the inactivity time, denoted by $n(t)$, is simply the amount of time since the last movement detected by any of the PIR sensors until t, given that the flat is occupied. When the flat is empty at t, we make the convention that $n(t)$ is *undefined*.

3) Per Region Dwell Time: At any time t, the dwell time at region r, denoted by $d_r(t)$, where $r \in \{1, 2, 3, 4\}$[c], is simply the amount of time since the first movement detected by the PIR sensor at region r until t given that the flat is occupied and that the resident is still in region r. When the resident is not in region r at t, we say that $d_r(t)$ is *undefined*.

While inactivity time had been the subject of several studies [6], [9], none have considered the use of region-specific dwell times. To aid us in the development of our scheme in

the next section, we define the notion of an *event* that will subsume both of the above quantities.

Definition 1 (Event). *An event E refers to an uninterrupted inactivity or dwell time and has duration $\tau_E^{\mathrm{e}} - \tau_E^{\mathrm{s}}$ where τ_E^{e} and τ_E^{s} are the end and start times, respectively. An event instance is delimited by undefined value, i.e., prior to τ_E^{s} and immediately after τ_E^{e}, the variable is undefined. In the case of inactivity, an event instance can also be delimited by activity.*

IV. DETECTING UNUSUAL INACTIVITY AND DWELL TIMES

We shall now proceed to discuss the key contribution of this paper which is the generation of dynamic alert thresholds that is personalized for every elderly resident. The proposed scheme, which we call Dwell Time-enhanced Dynamic Threshold (DTDT) can be employed to detect unusually long inactivity or dwell time durations. Every region in the house is associated with a dwell time threshold, while for the entire house, an inactivity time threshold is obtained.

A. Days and Epochs

Similar to existing work [6], [9], [11], we analyze the sensor information on a day-to-day basis. This is reasonable since individuals are likely to have distinct daily routines or activities that are amenable to learning.

We divide a 24-hour period into equal epochs, denoted by k, where $k = 1, 2, 3, \ldots, K$ and K is the number of epochs per day. To be more precise, we define epoch k to be of the duration within a half-closed interval $(t_k^{\mathrm{s}}, t_k^{\mathrm{e}}]$, where t_k^{s} is the start of the interval and t_k^{e} is the end of the interval. As will be elaborated later, the division of time into epochs is necessary for limiting the storage and computational complexity of our scheme.

Definition 2 (Inactivity and Dwell Time). *For every epoch k on day j, we define the following important quantities:*
- *$N_j(k)$: the inactivity time or duration; and*
- *$D_j^r(k)$: the dwell time at region r.*

Unlike the quantities $n(t)$ and $d_r(t)$ which can be naturally obtained, there are several issues that are immediate pertaining to the determination of $N_j(k)$ and $D_j^r(k)$.

1) Multiple Events Per Epoch: Consider the case where there are multiple events in epoch k. One simple approach is to sum up all the event durations and use the sum to indicate $N_j(k)$ or $D_j^r(k)$ accordingly. Note however that this approach does not aid us in characterizing the individual event durations at k. Since the ultimate aim is to detect unusually long event durations, then using the maximum event duration makes more sense. More formally, suppose that the resident has been inactive for durations $X_1, X_2, X_3, \ldots, X_m$ on day j at epoch k, then

$$N_j(k) := \max(X_1, X_2, X_3, \ldots, X_m).$$

Likewise, if the resident has visited region r with dwell time durations $Y_1, Y_2, Y_3, \ldots, Y_n$ on day j at epoch k, then

$$D_j^r(k) := \max(Y_1, Y_2, Y_3, \ldots, Y_n).$$

Threshold	Description
$\mathcal{N}_j(k)$	Inactivity threshold at epoch k on day j
$\mathcal{D}_j^r(k)$	Dwell time threshold at epoch k on day j for every region r

2) Events That Extend Beyond An Epoch: There are three possible cases for this. In the first case, the event E that started at time τ_E^{s} in an epoch prior to k terminates at time τ_E^{e} in epoch k. Then if the event corresponds to inactivity and supposing that in the same epoch, the resident has been inactive for durations $X_1, X_2, X_3, \ldots, X_m$, we have

$$N_j(k) := \max(\tau_E^{\mathrm{e}} - \tau_E^{\mathrm{s}}, X_1, X_2, X_3, \ldots, X_m).$$

If E is a dwell time in region r, and supposing that in the same epoch, the resident has visited r for durations $Y_1, Y_2, Y_3, \ldots, Y_n$, we have

$$D_j^r(k) := \max(\tau_E^{\mathrm{e}} - \tau_E^{\mathrm{s}}, Y_1, Y_2, Y_3, \ldots, Y_n).$$

In the second case, the event E continues from the preceding epoch $k-1$ and continues to the next epoch $k+1$. This case is straightforward since there is only a single event instance. If the event corresponds to an inactivity time,

$$N_j(k) := t_k^{\mathrm{e}} - \tau_E^{\mathrm{s}},$$

where t_E^{e} is the time that epoch k ends and τ_E^{s} is the start of the event while if the interval is a dwell time at region r, then

$$D_j^r(k) := t_k^{\mathrm{e}} - \tau_E^{\mathrm{s}}.$$

In the third case, the event starts at time τ_E^{s} in epoch k and continues to the next epoch $k+1$. If the interval is an inactivity time and supposing that in the same epoch, the resident has been inactive for durations $X_1, X_2, X_3, \ldots, X_m$, we have

$$N_j(k) := \max(t_k^{\mathrm{e}} - \tau_E^{\mathrm{s}}, X_1, X_2, X_3, \ldots X_m).$$

If the interval is a dwell time in region r, and supposing that in the same epoch, the resident has visited r for durations $Y_1, Y_2, Y_3, \ldots, Y_n$, we have

$$D_j^r(k) := \max(t_k^{\mathrm{e}} - \tau_E^{\mathrm{s}}, Y_1, Y_2, Y_3, \ldots, Y_n).$$

B. Adaptive Thresholds

We will derive a global (residence-wide) inactivity threshold and region-specific dwell time thresholds, as enumerated in Table I. Note that for the former, we can use existing schemes such as the algorithm proposed by Cuddihy *et al* [6]. We therefore focus our attention in the derivation of region-specific dwell time thresholds.

1) Adaptation Window: To adapt to the activity patterns of the resident, the derivation of $\mathcal{D}_j^r(k)$ must consider $\mathcal{D}_i^r(k)$, for $i < j$. The length of historical data to be considered, or the *adaptation window* W affects the performance of the threshold. If W is too large, the threshold will be slow to adapt whereas if W is too small, the threshold will exhibit instabilities and will be sensitive to daily variations.

2) Lag and Lead Window: By considering only $\mathcal{D}_i^r(k)$, for $j - W \leq i \leq j - 1$, this is tantamount to assuming that the elderly adheres to a strict living pattern. This may not reflect reality where it is possible for her to sleep/wakeup much earlier or later than usual. Likewise, she might bathe, cook, and have her meals much earlier or later than usual. To account for this possible shifts in daily activities, we include a *lag and lead window L*, such that in determining $\mathcal{D}_j^r(k)$, we consider $\mathcal{D}_i^r(l)$, for $l = k - L, \ldots, k - 1, k, k + 1, \ldots, k + L$.

Now, let

$$\mathbf{D}_j^r(k) = \{D_i^r(l) \mid j - W \leq i \leq j - 1, k - L \leq l \leq k + L\}.$$

As we can see, the elements of $\mathbf{D}_j^r(k)$ represent the epoch maxima or the so-called extreme values. We want to obtain a threshold $\mathcal{D}_j^r(k)$ such that it is greater than every element in $\mathbf{D}_j^r(k)$. Indeed, we want to exploit the underlying structure of $\mathbf{D}_j^r(k)$ in setting $\mathcal{D}_j^r(k)$. Assuming that the elements in $\mathbf{D}_j^r(k)$ are *i.i.d.* and belong to a distribution with cdf $G(x)$, then we want to find $\mathcal{D}_j^r(k)$ such that for any random value X taken from this distribution, $\mathsf{Pr}(X > \mathcal{D}_j^r(k))$ is *small* and *within our control*. From elementary probability,

$$\mathsf{Pr}(X > \mathcal{D}_j^r(k)) = 1 - \mathsf{Pr}(X \leq \mathcal{D}_j^r(k)) = 1 - G(\mathcal{D}_j^r(k)). \quad (1)$$

It turns out that since $\mathbf{D}_j^r(k)$ contains extreme values, its distribution can be modeled after the extreme value distribution [5]. Hence,

$$G(x) = \exp\left\{-\exp\left[-\left(\frac{x - \mu}{\sigma}\right)\right]\right\}, \quad (2)$$

where μ and σ are known as the *location* and *scale* parameters, respectively. These parameters can be obtained through maximum likelihood estimation using the data $\mathbf{D}_j^r(k)$ [5]. Letting p correspond to the probability of exceeding $\mathcal{D}_j^r(k)$, *i.e.*, $p = \mathsf{Pr}(X > \mathcal{D}_j^r(k))$, from (1) and (2) we obtain

$$G(\mathcal{D}_j^r(k)) = 1 - p = \exp\left\{-\exp\left[-\left(\frac{\mathcal{D}_j^r(k) - \mu}{\sigma}\right)\right]\right\}.$$

Solving for $\mathcal{D}_j^r(k)$, we obtain the following closed-form solution:

$$\mathcal{D}_j^r(k) = \mu - \sigma \ln(-\ln(1 - p)), \quad (3)$$

where $\ln(\cdot)$ denotes the natural logarithm function. The main attraction of (3) is that it provides us with a single mechanism for controlling the performance of our thresholding scheme, that is through p. Intuitively, we want p to be as low as possible to minimize false alarms. However this will result in a very high threshold and hence, very high detection latency.

We note that compared to the global threshold that is always available, region-specific thresholds may not be available for certain regions at certain times. For instance, if a resident has never visited the kitchen between 12:00–3:00 a.m. (in the past few days equivalent to the adaptation window), then there would be no region-specific threshold for the kitchen at epochs that fall within 12:00–3:00 a.m.
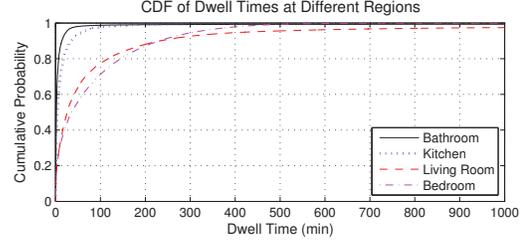

Fig. 3. CDF of dwell times at different regions of the house, for all the 20 participants combined.

3) Alert Threshold: The alert threshold to be applied on day j at time t depends on the location of the elderly resident at that instant, the epoch where t belongs, and the availability of region-specific threshold. For instance, if the resident is in the bathroom on day 10 at 12:00 a.m. (which is in epoch 1), then we first determine if the region-specific threshold $\mathcal{D}_{10}^4(1)$ is available. If it is, then we use it as the alert threshold. Otherwise, we use the global threshold $\mathcal{N}_{10}(1)$ as the alert threshold. Generalizing this, the alert threshold for day j at epoch k, given that the resident is in region r, is given by

$$\mathcal{T}_j(k) = \begin{cases} \mathcal{D}_j^r(k), & \text{if the threshold is available} \\ \mathcal{N}_j(k), & \text{otherwise.} \end{cases}$$

The disadvantage of the above formulation is that since $\mathcal{D}_j^r(k)$ refers to the dwell times at specific regions, it may turn out to be higher than $\mathcal{N}_j(k)$ at certain times in certain regions. For instance, we have observed that when the resident is asleep in the bedroom at night, the PIR sensor still periodically detects movements. This results in shorter inactivity durations. To mitigate this issue, we therefore set the threshold to be the lower value between $\mathcal{D}_j^r(k)$ and $\mathcal{N}_j(k)$, that is

$$\mathcal{T}_j(k) = \min[\mathcal{D}_j^r(k), \mathcal{N}_j(k)]. \quad (4)$$

V. EVALUATION

To determine the performance of DTDT, we perform trace-driven simulations using the 6-month (184-day) SHINESeniors sensor data from March 1 to August 31. Of the current 50 elderly participants, we have selected 20 for the following reasons: (*i*) 20 of the participants joined at much later dates after March 1, and (*ii*) data from 10 of the participants who joined before March 1 have several days of missing readings due to connectivity issues. Fig. 3 shows the CDF of the dwell times at different regions of the house, with the bathroom and kitchen showing significantly lower dwell times than both the living room and bedroom.

For every participant, we have segmented the data such that 30 days are used for training and the remaining days are used for testing. To maximize the use of the data, we have randomly chosen different contiguous 30-day segments from the 184-day data for training, and the rest for testing. A particular data segmentation constitutes 1 seed. This approach is similar to the simulations performed in [6].

As mentioned in Section IV-B, DTDT can use existing schemes to compute the global threshold $\mathcal{N}_j(k)$. In this study,
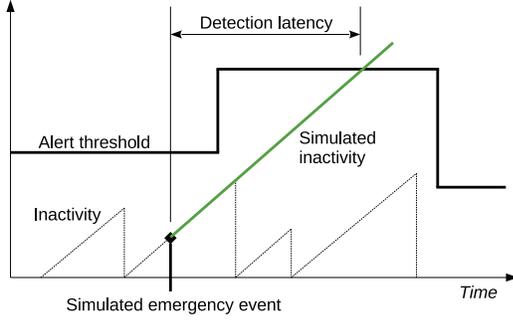
Fig. 4. Occurrence of simulated emergency event that causes non-movement and its detection latency, *i.e.*, the time from event occurrence until its detection. The y-axis denotes cumulative duration. After the simulated event happens, the inactivity duration keeps on increasing to simulate the lack of movement. When the inactivity duration crosses the alert threshold, an alert is generated to indicate the detection of the simulated event.

we have used the Automatic Inactivity Detection (AID) [6] to obtain $\mathcal{N}_j(k)$. The number of epochs K is set to 48.

A. Performance Metrics

Our goal in this paper is to improve the sensitivity of the system while ensuring that the false alarm rate is within specified bounds. Hence, the two key performance metrics of interest are the *detection latency* and *false alarm rate per week*. Note the opposing nature of these two metrics: reducing detection latency results in worse false alarm rate, while lowering false alarm rate yields higher detection latency.

Obtaining the false alarm rate is straightforward. After calculating the alert threshold $\mathcal{T}_j(k)$, we simply count the number of times that the inactivity time $n(t)$ have exceeded $\mathcal{T}_j(k)$ and divide this by the number of weeks. This is justified since the 6-month inactivity data that was used did not contain actual emergency so any alert could be considered as false.

To measure the detection latency, we have simulated "emergency events" in different regions of the house. For every seed, we have randomly picked 100 instances (chosen from a uniform distribution) where the resident is in region r and simulated emergency event that results in non-movement. That is, if the resident is in region r at time t with inactivity time $n(t)$, then from then on, $n(t)$ will keep on increasing (to simulate non-movement) until it exceeds the alert threshold. The detection latency is simply the time from the simulated emergency event until $n(t)$ exceeds the alert threshold. Fig. 4 illustrates the emergency event simulation and detection latency.

B. Effect of Exceedance Probability

The performance of DTDT can be tuned using the exceedance probability p. Recall that low p would yield low false alarm rate but high detection latency while high p would result in low detection latency but high false alarm rate. To see if this is indeed the case, we conducted simulations in Matlab where p is varied from 0.01 to 0.1. Figs. 5(a) and 5(b) show the average false alarm per week and detection latency as p is varied from 0.01 to 0.1. In Fig. 5(b), a line plot corresponds to a particular location of simulated emergency event.
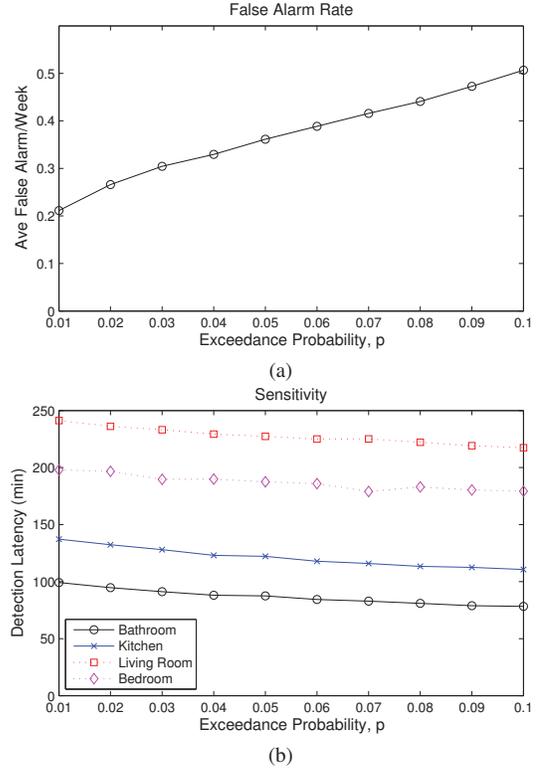

(a)

(b)

Fig. 5. False alarm rate and detection latency of DTDT as a function of p.

We can observe from Fig. 5(a) that as p increases, the false alarm rate increases. This is expected since from its formulation (see Eq. (3)), the threshold decreases as p increases. Hence, given the same inactivity data, a lower threshold would result in more instances of it being exceeded.

With respect to the detection latency, we can see that from Fig. 5(b), the average latency shows noticeable decrease (by around 20 minutes in all locations) as p increases. This result is anticipated, since higher p implies lower threshold which eventually entails shorter detection delay.

A notable feature of Fig. 5(b) are the distinct magnitudes of the latency for different emergency event locations, with bathroom showing the lowest and living room showing the highest. This observation is mainly due to the different dwell times at these different locations. As mentioned, DTDT exploits dwell times to shorten the detection latency, hence for regions with high dwell times such as living room and bedroom, the resulting latency are also high.

C. Performance Comparison

We compare the performance of DTDT with two of the state-of-the-art dynamic alert thresholding schemes, namely, AID [6] and the algorithm proposed by Moshtaghi *et al.* [8]. The latter scheme was actually designed to exploit region-based inactivity data, but simulations show that employing region-specific inactivity data result in worse performance [8]. Thus, we have configured the algorithm by Moshtaghi *et al.* to use global inactivity data similar to AID.

We performed simulations in Matlab and to ensure fairness, we modified the respective scheme parameters so that the

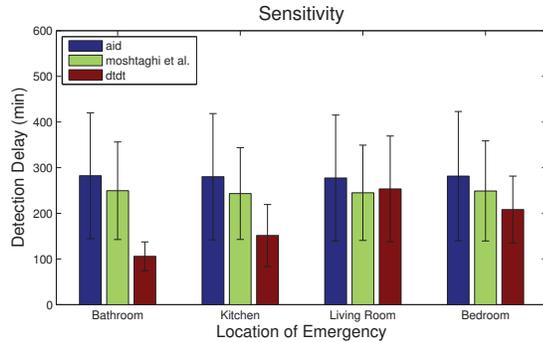|	AID	Moshtaghi *et al.*	DTDT
Average	0.289	0.279	0.286
Standard Deviation	0.120	0.140	0.175

Fig. 6. Detection latency of simulated emergency events occurring in different regions of the house. The error bars indicate the 95% confidence intervals.

resulting false alarm rates were roughly the same for the three schemes. We fixed an objective of at most one false alarm per week on the average. Table II shows the average false alarm rate per week of the three schemes. The results show that DTDT has slightly higher standard deviation compared to the other two schemes.

Fig. 6 shows the detection latency of the simulated emergency events with respect to the region of occurrence, with the error bars signifying the 95% confidence intervals. Note that regardless of the region of emergency event occurrence, AID and Moshtaghi *et al.* show the same detection latency. This is expected since both schemes calculate their respective alert thresholds using the global inactivity data. Whereas, we can observe that DTDT shows different latency for different locations. Notably, DTDT shows significantly shorter latency compared to the other schemes, especially when emergency events happen in the bathroom or kitchen. Compared to AID, its latency is 182 and 129 minutes (3 and 2 hours) shorter for events occurring in the bathroom and kitchen, respectively. Compared to Moshtaghi *et al.*, its latency is better by 143 and 92 minutes (2.4 and 1.5 hours) for events occurring in the bathroom and kitchen, respectively. For events that occur in the living room and bedroom, DTDT shows comparable performance.

The performance advantage of DTDT can be attributed to its use of dwell time to lower the alert threshold. It shows better performance in the bathroom and kitchen because residents do not tend to stay long in these locations. It does not show significant improvement in the living room and bedroom because residents tend to dwell longer in these locations.

VI. CONCLUSION AND FUTURE WORK

The use of PIR sensors to monitor the condition and well-being of seniors is one of the more acceptable in-home sensor technologies because of their unobtrusiveness. These sensors enable the monitoring of inactivity, and several algorithms have been proposed to detect unusually long periods of inactivity. In this paper, we have proposed Dwell Time-enhanced Dynamic Threshold (DTDT), a scheme for computing adaptive alert thresholds that exploit region-specific dwell time to reduce the detection latency. Using extreme value theory, we have obtained a closed form expression for the region-specific alert thresholds. We have performed simulations using real sensor data to evaluate DTDT and compare it with state-of-the-art schemes AID and the algorithm by Moshtaghi *et al.* Results show that DTDT shows significantly lower detection latency in regions with short dwell times (bathroom and kitchen) while maintaining the same false alarm rate.

We are currently studying the use of other types of unobtrusive sensors to improve the sensitivity of the system. We are also looking at other anomaly detection schemes to improve the false alarm rate and detection latency.

REFERENCES

[1] Aging in place: A state survey of livability policies and practices, Dec. 2011. AARP Public Policy Institute and National Conference of State Legislatures.

[2] World population ageing, 2013. United Nations Department of Economic and Social Affairs, Population Division.

[3] K. Addae-Dapaah and G. K. M. Wong. Housing and the elderly in singapore–financial and quality of life implications of ageing in place. *Journal of Housing and the Built Environment*, 16(2):153–178, 2001.

[4] A. Arcelus, M. H. Jones, R. Goubran, and F. Knoefel. Integration of smart home technologies in a health monitoring system for the elderly. In *Proc. International Conference on Advanced Information Networking and Applications Workshops*, volume 2, pages 820–825. IEEE, 2007.

[5] S. Coles. *An Introduction to Statistical Modeling of Extreme Values*. Springer, 2001.

[6] P. Cuddihy, J. Weisenberg, C. Graichen, and M. Ganesh. Algorithm to automatically detect abnormally long periods of inactivity in a home. In *Proc. ACM SIGMOBILE International Workshop on Systems and Networking Support for Healthcare and Assisted Living Environments*, pages 89–94, 2007.

[7] M. Larizza, I. Zukerman, F. Bohnert, R. Russell, L. Busija, D. Albrecht, and G. Rees. Studies to determine user requirements regarding in-home monitoring systems. In J. Masthoff, B. Mobasher, M. Desmarais, and R. Nkambou, editors, *User Modeling, Adaptation, and Personalization*, volume 7379 of *Lecture Notes in Computer Science*, pages 139–150. Springer Berlin Heidelberg, 2012.

[8] M. Moshtaghi, I. Zukerman, D. Albrecht, and R. Russell. Monitoring personal safety by unobtrusively detecting unusual periods of inactivity. In S. Carberry, S. Weibelzahl, A. Micarelli, and G. Semeraro, editors, *User Modeling, Adaptation, and Personalization*, volume 7899 of *Lecture Notes in Computer Science*, pages 139–151. Springer Berlin Heidelberg, 2013.

[9] M. Moshtaghi, I. Zukerman, D. Albrecht, and R. Russell. Monitoring personal safety by unobtrusively detecting unusual periods of inactivity. In S. Carberry, S. Weibelzahl, A. Micarelli, and G. Semeraro, editors, *User Modeling, Adaptation, and Personalization*, volume 7899 of *Lecture Notes in Computer Science*, pages 139–151. Springer Berlin Heidelberg, 2013.

[10] R. Planinc and M. Kampel. Detecting unusual inactivity by introducing activity histogram comparisons. In *Proc. International Conference on Computer Vision Theory and Applications*, volume 2, pages 313–320, Jan. 2014.

[11] J. Saives, C. Pianon, and G. Faraut. Activity discovery and detection of behavioral deviations of an inhabitant from binary sensors. *IEEE Trans. Automation Science and Engineering*, 12(4):1211–1224, Oct. 2015.

[12] N. K. Suryadevara and S. C. Mukhopadhyay. Wireless sensor network based home monitoring system for wellness determination of elderly. *Sensors Journal, IEEE*, 12(6):1965–1972, 2012.

[13] B. Yuan and J. Herbert. Non-intrusive movement detection in cara pervasive healthcare application. In *Proc. International Conference on Wireless Networks (WORLDCOMP)*, volume 11, pages 360–366, 2011.